Numerical Investigation on Contactless Methods for Identifying Defects in High-Temperature Superconducting Film*)

Teruou TAKAYAMA, Atsushi KAMITANI[1)] and Hiroaki NAKAMURA[2)]

Department of Informatics, Yamagata University, Yonezawa 992-8510, Japan
[1)]*Graduate School of Science and Engineering, Yamagata University, Yonezawa 992-8510, Japan*
[2)]*National Institute for Fusion Science, Toki 509-5292, Japan*

(Received 25 November 2014 / Accepted 6 April 2015)

A numerical method has been developed for analyzing the shielding current density in a high-temperature superconducting (HTS) film containing multiple cracks. By using the method, the inductive method and the scanning permanent magnet method for contactlessly measuring the critical current density has been successfully reproduced, and the identifiability of the multiple cracks in the HTS film has been investigated. The results of computations show that, when the cracks are separated from each other, the multiple cracks can be detected individually in the two types of the contactless method. On the other hand, if the crack is pretty close to the interface, the multiple cracks is considered as a single crack. However, the crack position can be detected collectively. Therefore, the contactless methods is useful method for detecting the multiple cracks in an HTS film.

Keywords: multiple crack, critical current density, finite element analysis, numerical simulation, high-temperature superconducting film

DOI: 10.1585/pfr.10.3401059

1. Introduction

A measurement of a critical current density j_C is essential for designing high-temperature superconducting (HTS) devices such as a MRI, an HTS cable, and a linear motor car. An Inductive method [1,2] for measuring a critical current density j_C is employed as the crack detection in an HTS sample. Kim experimentally investigated the detectability of a crack from observing the V_3-I_0 curves [3]. He found that the threshold current of I_0 decreases if the coil approaches the crack. This result means that the crack can be detected by the inductive method.

As an novel method, Ohshima *et al.* proposed a standard permanent magnet method [4]. This method is used for a crack detection. In the method, while moving a permanent magnet above an HTS film, an electromagnetic force F_z acting on the film is monitored. They found that when the magnet approached the crack, the maximum repulsive force F_M decreases. Consequently, the crack can be detected by measuring F_M. However, it has time-consuming because to the evaluation of F_M at each measurement point.

For the purpose of j_C-measurements with a high speed, Hattori *et al.* have recently proposed a scanning permanent magnet method [5]. A magnet is placed in relation to a film surface at a constant distance between an HTS surface and the magnet bottom, and it is moved in the direction parallel to the surface. As a result, although the j_C-measurement speed is higher than the standard method, they have not yet been applied scanning method to the crack detection.

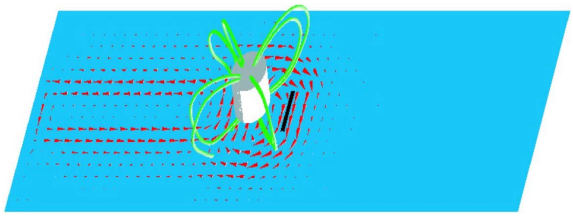

Fig. 1 Time evolution of the magnetic flux lines and the shielding current density in an HTS film with a single crack when a magnet is moving from the left edge to the right edge. An important point is that you can see an animation on a PDF file by clicking this figure only when you download and install the Adobe Acrobat Reader and the QuickTime on your computer.

In the previous study, we develop a numerical code for analyzing the time evolution of a shielding current density in an HTS film with a single crack [6–8]. By using the code, we obtain the time evolution of the magnetic lines and the shielding current density is illustrated for a typical case in Fig. 1. In this figure, the green lines and the arrows indicate the magnetic flux lines and the flow of a shielding current density, respectively. The blue plane, the gray cylinder and the black line show the HTS film, the permanent magnet, and a single crack, respectively. In addition, we investigate the detectability of the scanning permanent magnet/inductive methods. The results of the com-

author's e-mail: takayama@yz.yamagata-u.ac.jp
*) This article is based on the presentation at the 24th International Toki Conference (ITC24).

putations show that the single crack can be detected with high speed and high accuracy by combining the inductive method and the scanning one [8].

We see from this figure that a shielding current density $\boldsymbol{j}$ flows along the crack. Furthermore, $\boldsymbol{j}$ remains in the film after passing through the magnet. The magnetic flux lines are greatly changed under the influence of the crack and the edge.

The purpose of the present study is to investigate the identifiability of multiple cracks by the contactless methods by modifying an above mentioned numerical code.

2. Governing Equations

In the present study, we suppose that an HTS film contains m pieces of cracks. A rectangle cross-section Ω of the film has not only the outer boundary C_0 but also the inner boundaries C_k ($k = 1, 2, \cdots, m$). Moreover, $\boldsymbol{n}$ and $\boldsymbol{t}$ on C_k are a normal unit vector and a tangential unit vector.

As usual, we use the Cartesian coordinate system $\langle O : \boldsymbol{e}_x, \boldsymbol{e}_y, \boldsymbol{e}_z \rangle$ (see Fig. 2): z-axis is parallel to the thickness direction. Also, it should be noted that the origin O is chosen at the centroid of an HTS in the scanning permanent magnet method. On the other hand, O is taken at the center of an HTS upper surface in the inductive method. In terms of the coordinate system, the symmetry axis of the magnet and the coil can be expressed as $(x, y) = (x_A, y_A)$.

As is well known, a closely relationship between a shielding current density $\boldsymbol{j}$ an electric field $\boldsymbol{E}$ can be written as the J-E constitutive equation

$$\boldsymbol{E} = E(|\boldsymbol{j}|)\left(\frac{\boldsymbol{j}}{|\boldsymbol{j}|}\right), \quad E(j) = E_C\left(\frac{j}{j_C}\right)^N.$$

Here, j_C, E_C, and N are the critical current density, the critical electric field, and a positive value, respectively. As a function $E(j)$, we adopt the power law for characterizing a HTS property.

Similar to the previous study, we use the thin-layer approximation [9]: the thickness of an HTS film is thin enough so that the shielding current density $\boldsymbol{j}$ can hardly flow in the thickness direction. From this approximation it is follows that $\boldsymbol{j} = (2/b)(\nabla S \times \boldsymbol{e}_z)$, where a scalar function $S(\boldsymbol{x}, t)$ and its time evolution is governed by the following integro-differential equation [9]:

$$\mu_0 \partial_t(\hat{W}S) + \boldsymbol{e}_z \cdot (\nabla \times \boldsymbol{E}) = -\partial_t \langle \boldsymbol{B} \cdot \boldsymbol{e}_z \rangle. \quad (1)$$

Here, the square bracket $\langle \ \rangle$ denotes an average operator over the thickness, and $\boldsymbol{B}$ is an applied magnetic field. The explicit form of $\hat{W}$ is given in Ref. [9].

Applying the initial condition $S = 0$ at $t = 0$ to (1), we assume the three boundary conditions: $S = 0$ on C_0, $\partial S/\partial s = 0$ on C_k, and $h_k(\boldsymbol{E}) \equiv \oint_{C_k} \boldsymbol{E} \cdot \boldsymbol{t} ds = 0$, where s is an arclength along C_k. By solving the initial-boundary-value problem of (1), we can determine the time evolution of the shielding current density $\boldsymbol{j}$ in an HTS film with the multiple cracks.

As the discretization methods, we apply the finite element method and the backward Euler method to the initial-boundary-value problem of (1). The problem is reduced to the nonlinear boundary-value problem, and it is transformed by simultaneous linear equations by using the Newton method and virtual voltage method [10].

Incidentally, we adopt Hitachi SR16000 XM1 as the numerical computations. In the computers, the matrix calculation for the numerical libraries (MATRIX/MPP) is implemented. We use the HDLGEM subroutine to solve simultaneous linear equations in the initial-boundary-value problem of (1). As a result, the CPU time is about 92 times faster than before the implementation of the above subroutine.

Throughout the present study, the physical and geometrical parameters of the HTS film are fixed as follows: $l = 30$ mm, $w = 12$ mm, $b = 1\,\mu$m, $j_C = 1$ MA/cm^2, $E_C = 1$ mV/m, $N = 20$.

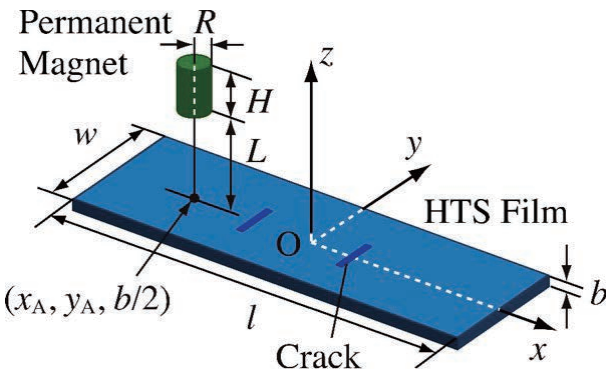

Fig. 2 A schematic view of a scanning permanent magnet method.

3. Identifiability of Multiple Cracks by Using Contactless Methods

In this section, we numerically investigate the identifiability of the multiple cracks by using the two types of the contactless methods for measuring a critical current density j_C. In the present study, the number m of cracks are $m = 3$, and three cracks are denoted by C_1, C_2, and C_3 (see Fig. 3). The shape of two cracks, C_1 and C_3, is the line segment paralleled to the y-axis, and C_2 is the vertical line to the y-axis. The length of C_1, C_2, and C_3 is fixed as L_c. In

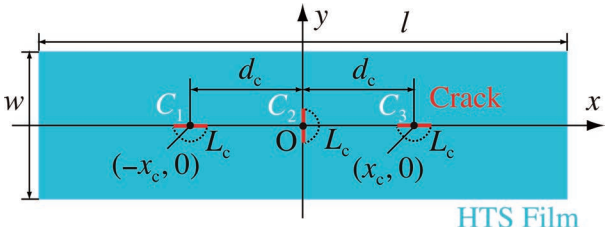

Fig. 3 The three cracks, C_1, C_2, and C_3, containing an HTS film.

addition, the center points $(x, y) = (\pm x_c, 0)$ and the origin in the xy-plane, and the distance between cracks is denoted by $d_c (\equiv 2x_c)$.

3.1 Scanning permanent magnet method

A cylindrical permanent magnet of radius R and height H is located above an HTS film, and a distance between a magnet bottom and a film surface is denoted by L. For characterizing the magnet strength, we use the magnitude B_F of a magnetic flux density at $(x, y, z) = (x_A, y_A, b/2)$ when the magnet is not moving.

In order to numerically assess the identifiability of the multiple cracks, the movement of the magnet is controlled by $x_A(t) = \pm(vt - l/2)$ $(\equiv x_\pm(t))$, where v is the magnitude of the scanning velocity. Specifically, the magnet is moved toward the right edge of the film for $x_A(t) = x_+(t)$. On the other hand, it is moved toward the left edge of the film for $x_A(t) = x_-(t)$.

The parameters in this subsection are fixed as follows: $R = 1$ mm, $H = 2$ mm, $B_F = 0.1$ T, $v = 30$ cm/s.

Although an electromagnetic force F_z acts on an HTS film by moving the magnet, it is difficult to detect the multiple cracks from the behavior of F_z. In order to identify cracks numerically, we adopt a defect parameter

$$d \equiv \mathrm{sgn}(\Delta F_z^+ \cdot \Delta F_z^-) \sqrt{|\Delta F_z^+ \cdot \Delta F_z^-|}. \tag{2}$$

Here, force deferences $\Delta F_z^\pm$ are determined form the difference between the electromagnetic forces $F_z^\pm$ with a crack and $F_z^\pm$ without a crack. In addition, the superscripts (+) and (-) denote the movement of the magnet for the case with $x_+(t)$ and $x_-(t)$, respectively.

In Fig. 4, we show the dependence of the defect parameter d on the magnet position x_A. We see from this figure that the value of d almost vanishes near the film edge, and we obtain d near the crack. For the case with $y_A = 3$ mm, d only appears near the crack C_2, whereas d affect the all cracks for $y_A = 0$ mm. Here, the defect parameter d is useful for the crack detection.

Finally, let us investigate the distribution of d for two types of the crack position. In Figs. 5 (a) and (b), we show the contour maps of the defect parameter d. We see from Fig. 5 (a) that three regions for $d > 0$ mN containing in each crack can be obtained. In addition, it is found that the largest value of d becomes around the both ends of the cracks C_1 and C_3. On the other hand, d does not increases at the end of C_2. From Fig. 5 (b), since the defect parameter d is forced near the cracks, it is difficult to identify crack individually. However, it is possible to estimate the approximate position and shape of the crack for this case.

3.2 Inductive method

A small M-turn coil of inner radius R_{in}, outer radius R, and height H is located just above an HTS film and an ac current $I(t) = I_0 \sin 2\pi f t$ flows in the coil. In addition, L denotes a distance between the coil bottom and the film

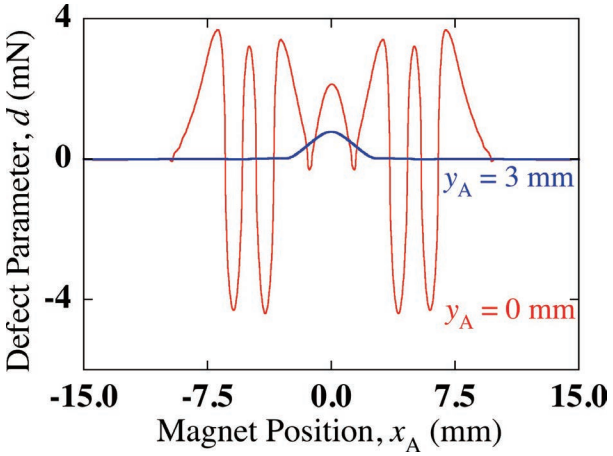

Fig. 4 Dependences of a defect parameter d on the magnet position x_A for the case with $d_c = 5$ mm.

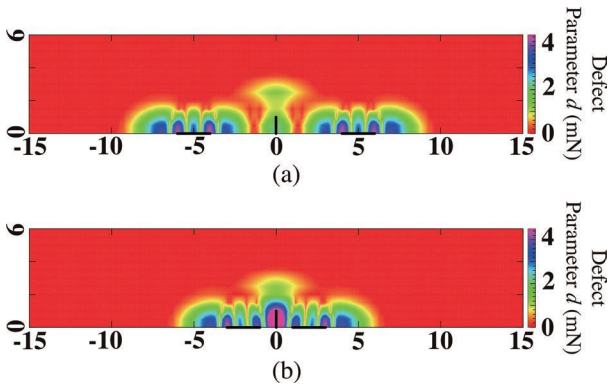

Fig. 5 Contour maps of a defect parameter $|d|$ for the case with (a) $d_c = 5$ mm and (b) $d_c = 2$ mm.

surface. As a result, a harmonic voltage V_n $(n = 1, 2, \cdots)$ is induced in the coil. A critical current density j_C can be estimated from a third-harmonic voltage V_3. In this subsection, we adopt the parameters as follows: $R_{in} = 0.75$ mm, $R = 1.25$ mm, $f = 1$ kHz, $M = 400$.

In order to determine j_C, it needs to evaluate a threshold current I_T when a third-harmonic voltage V_3 begins to develop in the coil. To this end, we use the conventional voltage criterion [2]

$$V_3 = 0.1 \text{ mV} \Leftrightarrow I_0 = I_T^*, \tag{3}$$

because it is difficult to determine I_T accurately. Here, I_T^* denotes an estimated value of the coil current I_0.

Let us first investigate the influence of the three cracks, C_1, C_2, and C_3, on a third-harmonic voltage V_3. In Fig. 6, we show V_3-I_0 curves for various x_A. From this figure, V_3 gradually develops above the certain value of I_0. Using the voltage criterion (3), we get $I_T^* = 158.8$ mA, 234.4 mA, and 261.1 mA for $x_A = 0$ mm, 2 mm, and 4 mm, respectively.

Next, let us investigate the detectability of multiple

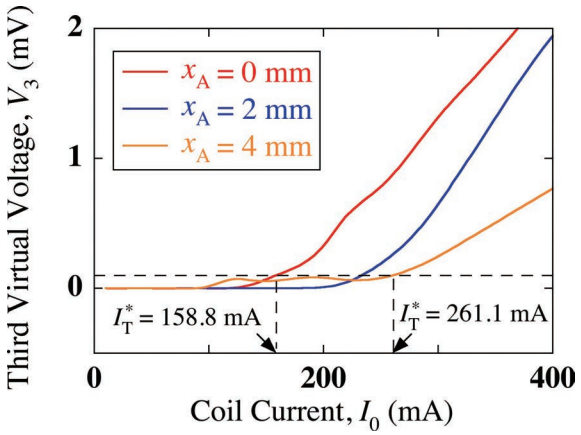

Fig. 6 V_3-I_0 curves for the case with $y_A = 0$ mm and $d_c = 5$ mm.

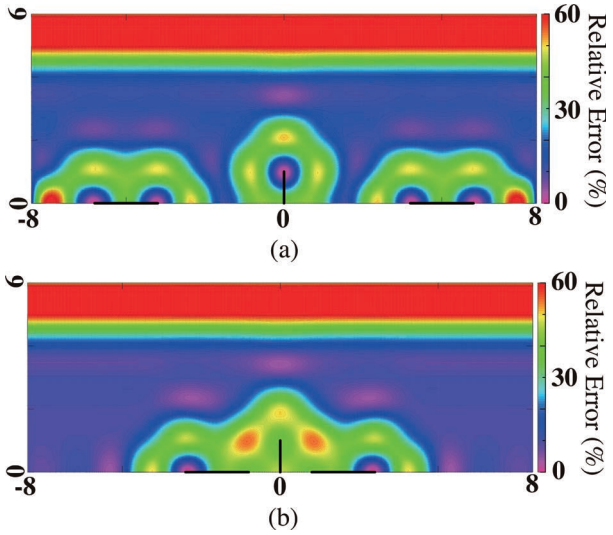

Fig. 7 Contour maps of the relative error e for the case with (a) $d_c = 5$ mm and (b) $d_c = 2$ mm.

cracks. To this end, a relative error is defined by

$$e \equiv |I_T^A - I_T^*|/I_T^A, \tag{4}$$

as a measure of the crack detection, where I_T^A is an analytic value of the threshold current determined from the Mawatari's theory [2].

In Figs. 7 (a) and (b), we show the contour maps of the relative error e for two types of the crack position. We see from Fig. 7 (a) that the distribution of the error e is contained in a region for $e > 0\%$ except for a HTS film edge and the both ends of cracks. Moreover, the value of e is $e = 0\%$ near the both ends of each crack. This result means that the crack position can be detected by examining the distribution of the relative error e. In Fig. 7 (b), although the values of e vanish near the left end of the crack C_1 and the right end of C_3, e at the top end of C_2 is about $e = 35\%$. Consequently, the multiple cracks is considered as a single crack, if the distance between the cracks is pretty close to the interface. However, the crack position can be detected collectively.

4. Conclusion

We have developed a numerical code analyzing the time evolution of the shielding current density in an HTS film containing the multiple cracks. By using the code, we numerically investigate the identifiability of the three cracks in the HTS film by the inductive method and the scanning permanent magnet method. Conclusions obtained in the present study are summarized as follows:

1. In the two types of the contactless method for measuring a critical current density, when the cracks are separated from each other, the multiple cracks can be detected individually. In detecting the cracks, the scanning method is used for a defect parameter determined from an electromagnetic force acting on an HTS film. In the inductive method, a distribution of a threshold current is adopted.
2. If the crack is pretty close to the interface, the multiple cracks is considered as a single crack. However, the crack position can be detected collectively.

Acknowledgment

This work was supported in part by Japan Society for the Promotion of Science under a Grant-in-Aid for Scientific Research (C) (No. 24560321, No. 26520204) and under a Grant-in-Aid for Encouragement of Scientists (No. 26919011). A part of this work was also carried out with the support and under the auspices of the NIFS Collaboration Research program (NIFS13KNTS025, NIFS13KNXN267). Moreover, the numerical computations were carried out on Hitachi SR16000 XM1 of the LHD Numerical Analysis Server in NIFS.

[1] J.H. Claassen, M.E. Reeves and R.J. Soulen, Jr., Rev. Sci. Instrum. **62**, 996 (1991).
[2] Y. Mawatari, H. Yamasaki and Y. Nakagawa, Appl. Phys. Lett. **81**, 2424 (2002).
[3] S.B. Kim, Physica C **463-465**, 702 (2007).
[4] S. Ohshima, K. Umezu, K. Hattori, H. Yamada, A. Saito, T. Takayama, A. Kamitani, H. Takano, T. Suzuki, M. Yokoo and S. Ikuno, IEEE Trans. Appl. Supercond. **21**, 3385 (2011).
[5] K. Hattori, A. Saito, Y. Takano, T. Suzuki, H. Yamada, T. Takayama, A. Kamitani and S. Ohshima, Physica C **471**, 1033 (2011).
[6] T. Takayama and A. Kamitani, IEEE Trans. Appl. Supercond. **23**, 9001107 (2013).
[7] A. Kamitani, T. Takayama and A. Saitoh, Physica C **504**, 57 (2014).
[8] T. Takayama and A. Kamitani, IEEE Trans. Appl. Supercond. **24**, 9001505 (2014).
[9] A. Kamitani and S. Ohshima, IEICE Trans. Electron. **E82-C**, 766 (1999).
[10] A. Kamitani, T. Takayama and S. Ikuno, Physica C **494**, 168 (2013).